ISSN 1392–1320 MATERIALS SCIENCE (MEDŽIAGOTYRA). Vol. 11, No. 1. 2005

Broadband Dielectric Spectroscopy of 0.2PMN-0.4PSN-0.4PZN Relaxors Ceramics

Jūras BANYS[1], Jan MACUTKEVIČ[1*], Algirdas BRILINGAS[1], Jonas GRIGAS[1], Karlis BORMANIS[2], Andris STENBERG[2]

[1]*Department of Radiophysics, Faculty of Physics, Vilnius University, Sauletekio 9, LT-2040 Vilnius, Lithuania;*
[2]*Institute of Solid State Physics, University of Latvia 8 Kengaraga str., 1063 Riga , Latvia*

Received 30 September 2004; accepted 07 October 2004

Results of broadband dielectric spectroscopy of $0.2PbMg_{1/3}Nb_{2/3}O_3$-$0.4PbSc_{1/2}Nb_{1/2}O_3$-$0.4PbZn_{1/3}Nb_{2/3}O_3$ ceramics are reported for $20 \le T \le 500$ K and 20 Hz $\le \nu \le$ 100 THz. Dielectric constant is very high (more 14000) in the vicinity of the peak. Anomalous broad dielectric relaxation has been observed near the temperature of the maximum permittivity, T_m (at 1 kHz). The distribution of relaxation times has been calculated directly from the dielectric spectra. Over the temperature of the maximum permittivity, T_m the distribution of the relaxation times is symmetrically shaped (Cole-Cole function is satisfactory to describe the dielectric response). At lower temperatures, the distribution of relaxation times becomes asymmetrically shaped. On further cooling the second maximum appears. Above 1 THz, the dispersion is determined by polar phonons active in infrared spectra. Their contribution to total static permittivity is substantial above the Burns temperature T_d and softening of the TO_1 optic mode accounts for the Curie-Weiss behaviour near T_d. Below T_d the ferroelectric soft mode hardens on cooling exhibiting no anomaly near temperature T_m of permittivity maximum. Around T_m the polar phonon contribution to permittivity is small compared to low-frequency permittivity due a strong dielectric dispersion which appears below T_d in the microwave and submilimetre region.
Keywords: ceramics, relaxors, dielectric dispersion, distribution of relaxation times, soft mode, Burns temperature.

INTRODUCTION

A special class of ferroelectric materials is known as relaxor ferroelectrics: they posses a high dielectric constant which changes very smoothly with temperature and they display a strong frequency dispersion. The high permittivity as well as other properties such as strong electrostriction make them suitable for industrial applications. Therefore research on the relaxor ferroelectric has two objects. One is to find high-performance materials for applications, and the other is to understand its polarization mechanism in theory. [1] Many physical models have been proposed to explain the behavior of the relaxor ferroelectrics, for example, the inhomogeneus microregion model, the micro-macro domain transition model, the superparaelectric model, the dipolar glass model and the glass model, the order-disorder model, the local electric field model, etc. [2] Most of the materials are lead-based perovskite with general formula $PbBB'O_3$.

The chemical disordered complex perovskite $PbSc_{1/2}Nb_{1/2}O_3$ (PSN) belongs to the relaxor family [3]. Among the different relaxor compounds, some of them exhibit no structural phase transition, like $PbMg_{1/3}Nb_{2/3}O_3$ (PMN), whereas some others exhibit a spontaneous relaxor-ferroelectric phase transition like $PbSc_{1/2}Nb_{1/2}O_3$ (PSN) or $PbSc_{1/2}Ta_{1/2}O_3$. Concerning stoichometric PSN, a first order phase transition between the relaxor and the ferroelectric phases has been observed to occur at about 380 K by the several authors. In the ferroelectric state the disordered PSN has a rhombohedral structure (space group R3m) with displacements of the Pb atoms along the threefold axis which have been found to be larger of the Sc/Nb atoms. In the paraelectric state, disordered PSN is cubic with space group $Pm\overline{3}m$. A high value of the isotropic displacement has been observed for lead atoms indicating the existence of a possible positional disorder, either static or dynamic.

PZN is a prototype relaxor ferroelectric [4]. It exhibits a large dielectric dispersion and a broad dielectric maximum that depend on both frequency and temperature. Earlier studies also reported a structural phase transition from cubic to rhombohedral symmetry which falls in the temperature region of the maximum of the dielectric peak. More recent studies only mentioned the coexistence of cubic and rhombohedral phases, with polar nanodomains growing into polar microdomains and their volume fraction increasing with decreasing temperature. Strain appears to play an important role in the nanodomain-to-microdomain phase transition, with therefore resembles a martensitic phase transformation. Both $PbMg_{1/3}Nb_{2/3}O_3$ (PMN) and the Zn analog (PZN) are disordered perovskites that posses fascinating dielectric properties. Each compound is characterized by quenched chemical disorder on the perovskite B site which is occupied by Mg^{2+} (or Zn^{2+}) and Nb^{5+} cations. It is well known that the mixed-valence character inherent to both PMN and PZN is required for the dielectric relaxation and "diffuse transition" in a temperature range around T_{max} (T_{max} = 265 K for PMN). Despite the similarities, PMN and PZN are surprisingly different. Whereas PZN is ferroelectric that transforms from a cubic to a rhombohedral phase at 410 K, PMN macroscopic symmetry remains cubic below T_{max} down to 5 K. [5] A spherical random bond – random field (SRBRF) model has recently by proposed [6] with incorporates the

*Corresponding author. Tel.: +370-5-2366077; fax.: +370-5-2366003.
E-mail address: *jan.macutkevic@ff.vu.lt* (J. Macutkevič)

peculiar properties of both dipole glass and random field models. In the framework of the SBRF model the main features of the dielectric behaviour of PMN and PMN-related relaxors have been described, in good agreement with experimental results. Nevertheless, the microscopic mechanism of relaxor behaviour is still a mater of discussion.

Frequency-dependent relaxor behaviour is observed in both order and disorder forms of (1–x)PMN-(x)PSN solid solution with $x \leq 0.6$. [6] At higher levels of substitution, the dielectric response is dependent on the degree of order: disorder samples are relaxors and ordered samples exhibit normal ferroelectric behaviour. Such behaviour is explained within a Bragg-Williams approach by employing the random layer model. In order to understand the peculiarities of PMN-PSN dielectric behaviour deeper they have developed a model according to which, at $x = 0.6$, the kind of polar region changes from the PMN (or Mg) – related to the PSN (or Sc) – related. They define the polar region as the lead ion being at the middle between Mg (Sc) ions and vibrating against its nearest Nb and O ions. The change of the kind of the polar region at $x = 0.6$ is due to the intersection of the sizes of the Sc-related and Mg related polar regions at this point.

Recently new ternary solid solutions $PbSc_{1/2}Nb_{1/2}O_3$-$PbZn_{1/3}Nb_{2/3}O_3$-$PbMg_{1/3}Nb_{2/3}O_3$ (PSN-PMN-PZN) have been synthesized by solid state reaction from oxides [7]. Ceramic sample have been obtained by both conventional and hot pressing technique. In the present work, the dielectric properties of 0.2PMN – 0.4PZN – 0.4PSN ceramics in very wide frequency 20 Hz $\leq \nu \leq$ 100 THz ant temperature $20 \leq T \leq 500$ K ranges is reported.

EXPERIMENTAL

The low-frequency dielectric response in the range of 20 Hz – 1 MHz was measured using a HP 4284 LCR meter. Dielectric measurements in the high-frequency range of 10 MHz – 1.25 GHz were performed using a computer controlled HF dielectric spectrometer. The dielectric parameters were calculated taking into account the electromagnetic field distribution in the sample [8]. In the frequency range 8 – 11 GHz have been used the waveguide automatic dielectric spectrometer. In all measurements the silver past has been used for contact. A custom made time-domain terahertz transmission was used to obtain the complex dielectric response in the range from 3 cm^{-1} to 30 cm^{-1} (90 – 900 GHz). The technique itself is suitable up to 80 cm^{-1}, but above 30 cm^{-1} the sample was opaque. This spectrometer uses a femtosecond Ti:sapphire laser and biased large aperture antenna from a low-temperature grown GaAs as THz emitter, and electro-optic sampling detection technique. This measuring technique is described in detail elsewhere [9]. A polished plane-parallel 80 μm thick disk with a diameter of 6 mm was studied. An Optistat CF cryostat with mylar windows (with thickness of 25 and 50 μm for the inner and outer windows, respectively) was used for measurements down to 20 K. Room and higher temperature infrared reflectivity spectra were obtained using a Fourier transform spectrometer (Bruker IFS 113v) in the frequency range of 20 – 3300 cm^{-1} (0.6 – 100 THz). Low-temperature measurements down to 20 K were performed up to 650 cm^{-1} only because the polyethylene windows used in the Optistat CF cryostat (Oxford Ins.) are opaque at higher frequencies. Pyroelectric deuterated triglicine sulfate detectors were used for the room and higher temperature measurements, while a highly sensitive, helium cooled (1.5 K) Si bolometer was used for low – temperature measurements. A disk-shaped sample with a diameter of 6 mm and thickness of 2 mm was investigated.

RESULTS AND DISCUSSIONS

The temperature dependence of real and imaginary parts of dielectric function for 0.2PMN-0.4PZN-0.4PSN ceramics at selected frequencies between 20 Hz and 300 GHz is shown in Fig. 1. The dielectric constant value around the peak is very high (more 14000). One can see that both ε' (T) and ε'' (T) maxima are shifted toward the lower temperatures as the measuring frequency decreased, and a strong dispersion of ε' and ε'' exist in the low temperature part of both dependencies. The frequency dependence of real and imaginary parts of dielectric function for 0.2PMN-0.4PZN-0.4PSN ceramics at selected temperatures between 250 K and 400 K is shown in Fig. 2. Anomalous broad dielectric relaxation have been observed near and down the temperature of maximum dielectric constant (at 1 kHz), but at higher temperatures the relaxation dispersion occurs in the higher frequency range of 10^7 to 10^{11} Hz like in most of order-disorder ferro-electrics. Obtained dielectric spectra were fitted with the empirical Cole-Cole formula:

$$\varepsilon = \varepsilon_{\infty R} + \frac{\Delta\varepsilon}{1+(i\omega\tau)^{1-\alpha}} , \qquad (1)$$

which reduces to the Debye type formula with α. In this equation $\Delta\varepsilon$ represents the strength of relaxator, τ is the mean Cole-Cole relaxation time, α is the relaxation time distribution parameter, $\varepsilon_{\infty R}$ is the contribution of all phonon modes and electronic polarization.

Calculated Cole-Cole dielectric dispersion parameters are present in Fig. 3. The parameter of Cole-Cole distribution of relaxation times α increased as the temperature decreased and is around 0.9 at $T < 270$ K also the distribution of relaxation times becomes very broad. The mean Cole-Cole relaxation time of present ceramic diverge with temperature according to Vogel-Fulcher law:

$$\tau = \tau_0 e^{\frac{E}{k(T-T_0)}} . \qquad (2)$$

The Vogel-Fulcher parameter is $\tau_0 = 6.27 \cdot 10^{-14}$, $T_0 = 241$ K, $E/k = 892$ K. The distribution of relaxation times has been calculated directly from the dielectric spectra according to formula:

$$\varepsilon^*(\nu) = \varepsilon_{\infty R} + \Delta\varepsilon \int_{-\infty}^{\infty} \frac{f(\tau) d\log\tau}{1+2\pi i \nu\tau} . \qquad (3)$$

The Tikhonov regularization method have been used. This method and calculation technique is described in detail elsewhere [10]. The Tikhonov regularization parameter 8 has been found as optimal. Obtained distribution of relaxation times for different temperatures is

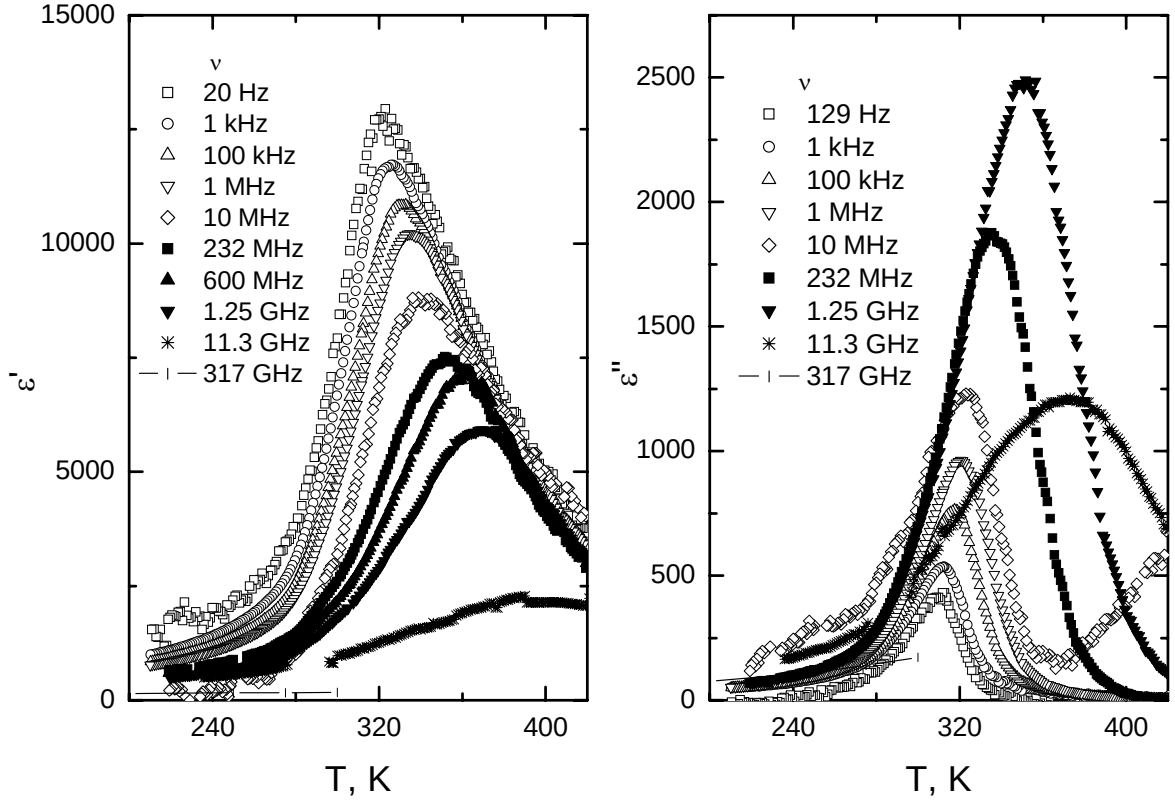

Fig. 1. The temperature dependence of the real part ε′ and imaginary part ε″ of the dielectric permittivity of 0.2PMN-0.4PZN-0.4PSN at different frequencies

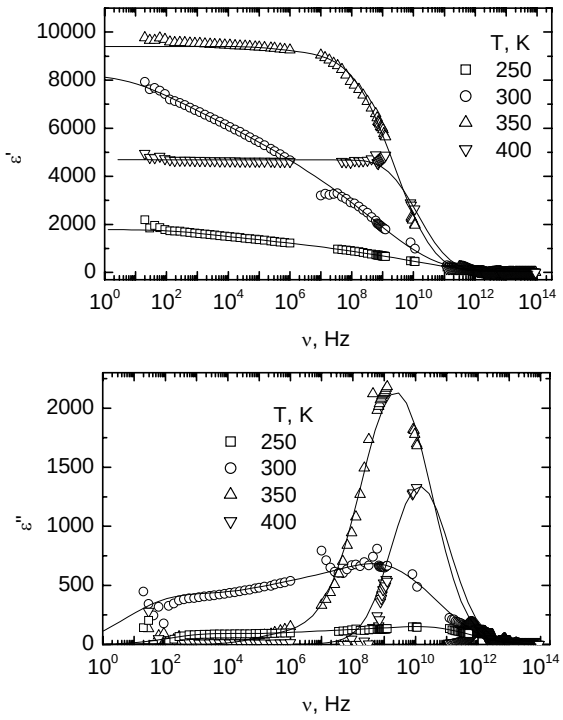

Fig. 2. Frequency dependence of ε′ and ε″ of 0.2PMN-0.4PZN-0.4PSN at different temperatures

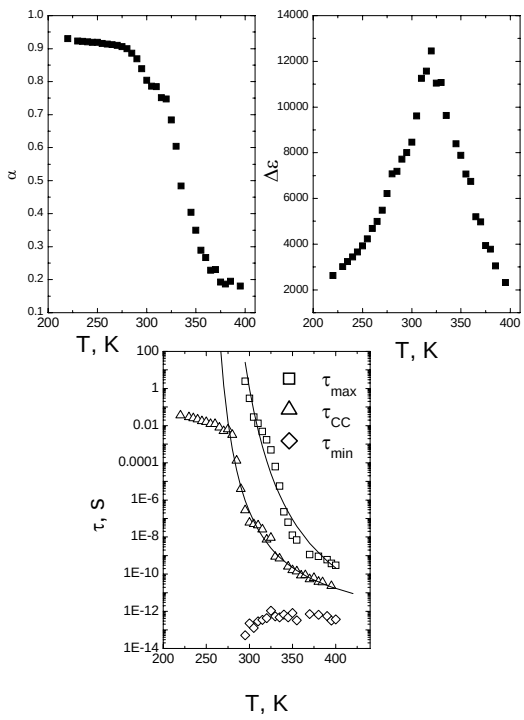

Fig. 3. Temperature dependence of dielectric dispersion parameters of 0.2PMN-0.4PZN-0.4PSN

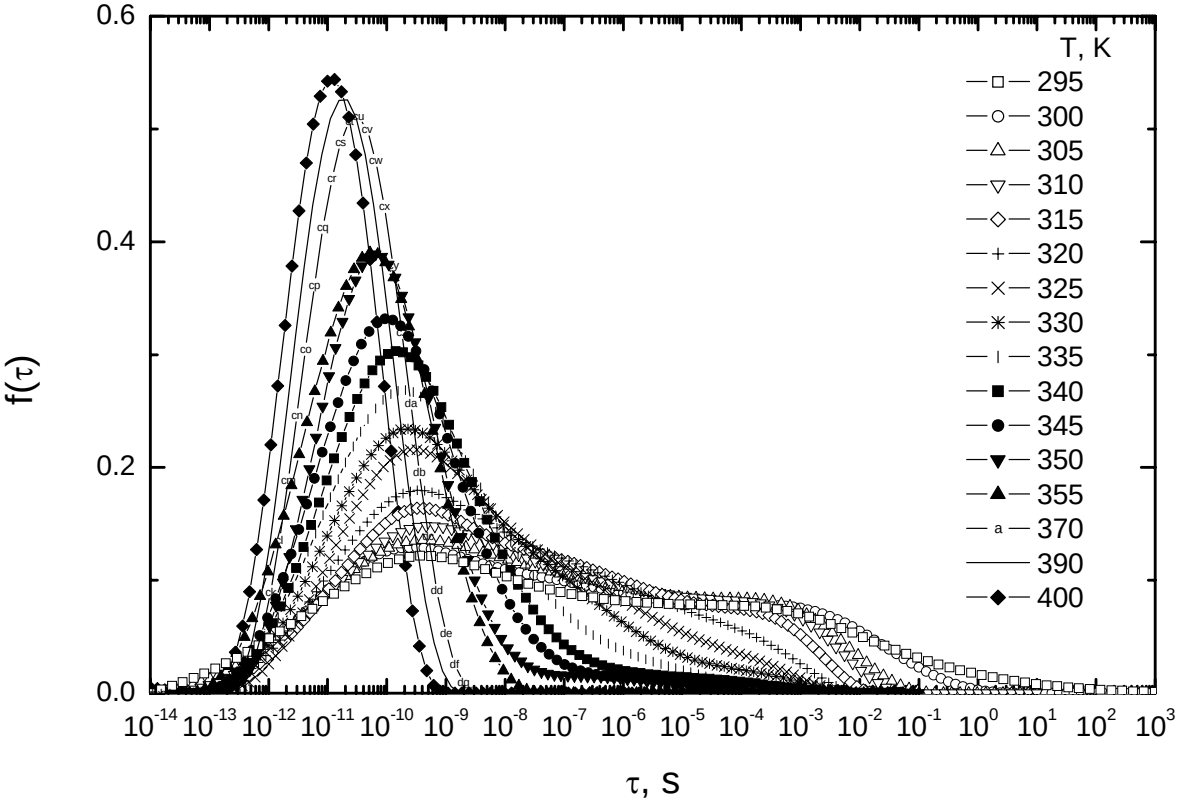

Fig. 4. The distribution of relaxation times of the 0.2PMN-0.4PZN-0.4PSN ceramics at several temperatures

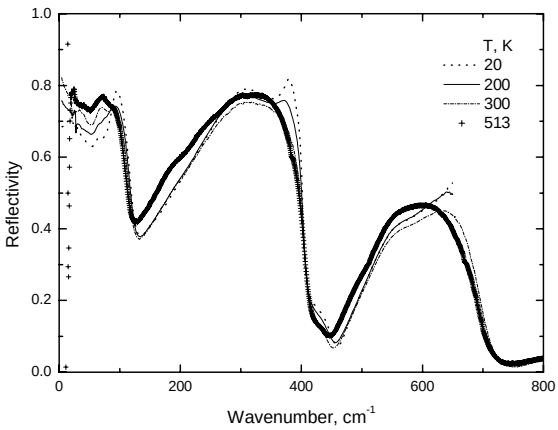

Fig. 5. The isothermal IR reflectivity spectra of 0.2PMN-0.4PZN-0.4PSN ceramics

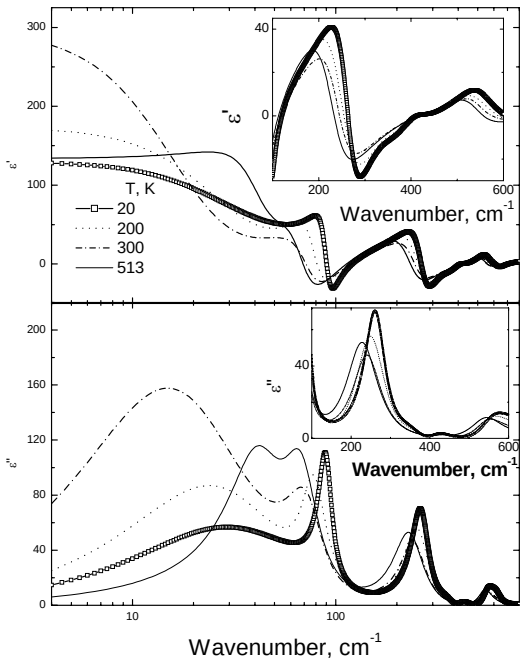

Fig. 6. The dielectric spectra obtained from IR reflectivity spectra

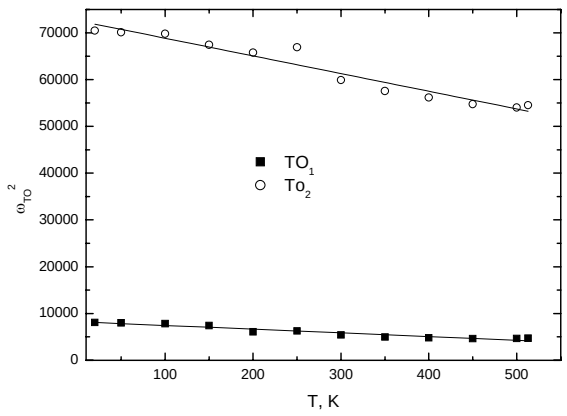

Fig. 7. The softening of TO_1 and TO_2 modes

present in Fig. 4. Over the temperature of the maximum permittivity, T_m the distribution of the relaxation times is symmetrically shaped (Cole-Cole function is satisfactory to describe the dielectric response). At lower temperatures, the distribution of relaxation times becomes asymmetrically shaped. On further cooling the second maximum appears.

The highest relaxation τ_{max} diverge according to Vogel-Fulcher law with parameters: $\tau_0 = 4.33 \cdot 10^{-16}$ s, $T_0 = 241$ K, $E/k = 2085$ K; the shortest relaxation times τ_{min} is about ps and independent from temperature (Fig. 3).

Isotermal IR and THz reflectivity spectra are shown in Fig. 5. The spectral range above 800 cm^{-1} is not shown because the reflectivity is flat at frequencies approaching the value given by the high-frequency permittivity ε_∞. One can see that two modes shifted to lower frequencies, as temperature increased. Below the freezing temperature T_0 the supplemental mode appears. IR and THz spectra were fitted simultaneously using a generalized-oscillator model of the factorised form of the complex permittivity:

$$\varepsilon^*(\omega) = \varepsilon_\infty \prod_j \frac{\omega_{LOj}^2 - \omega^2 + i\omega\gamma_{LOj}}{\omega_{TOj}^2 - \omega^2 + i\omega\gamma_{TOj}}, \quad (4)$$

where $\varepsilon^*(\omega)$ is related to reflectivity $R(\omega)$ by

$$R(\omega) = \left| \frac{\sqrt{\varepsilon^*(\omega)} - 1}{\sqrt{\varepsilon^*(\omega)} + 1} \right|, \quad (5)$$

ω_{TOj} and ω_{LOj} is the transverse and longitudinal frequency of the j-th mode, respectively, and γ_{TOj} and γ_{Loj} denote their corresponding damping constants.

The high-frequency permittivity ε_∞ resulting from electronic absorption processes was obtained from the frequency-independent RT reflectivity above the phonon frequencies. The temperature dependence of ε_∞ is usually very small and was neglected in our fit. The resulting real and imaginary parts of $\varepsilon^*(\omega)$ are shown in Fig. 6. The low-frequency part of the RT spectrum was fitted with an over damped oscillator. This fit does not explain the full value of the low frequency permittivity (Fig. 1) being still one order of magnitude higher due to the broad dispersion between low frequency and microwave frequency range (Fig. 2). The dispersion seen in the THz range is just the high frequency wings of this dispersion. For the IR spectra fitting we needed 6 (at temperature higher as freezing temperature T_0) and 7 (at temperature lower as freezing temperature T_0) phonon modes, which is inconsistent with the simple cubic structure of PMN, PSN and PZN (for PSN and PZN only in paraelectric phases) permitting only 3 IR active phonons in the spectrum. X-ray and neutron powder diffraction studies performed on PMN at 5 K revealed that the macroscopic symmetry is cubic; however the local symmetry is rhombohedral [5].

The correlation length of the polar rhombohedral clusters increases on cooling and saturates at about 10 nm at 5 K. The structure consists of two coexisting phases; the polar phase has been estimated as 20 % of the volume, the rest being a non-polar cubic phase. Rhombohedral structure allows for 16 IR active modes ($8A_1$+8E). We may not see all the modes, because some of them could be weak and/or they can be overlapped due to their finite widths. Nevertheless, the three main reflection bands stemming from the cubic phase are clearly seen. In present ceramics two soft modes (SM) TO_1 and TO_2 has been observed. The SM frequency (ω_{SM}) of the TO_1 and TO_2 in present ceramics shows pronounced temperature dependence and the TO_1 mode plays the role of the ferroelectric SM inside polar nanoclusters. TO_1 mode softens from ~90 cm^{-1} at 20 K to 68 cm^{-1} at 513 K (7) and TO_2 mode softens from ~265 cm^{-1} at 20 K to 233 cm^{-1} at 513 K. ω_{SM}^2 (T) obeys the Cochran law:

$$\omega_{SM}^2 = A(T_{cr} - T), \quad (6)$$

where A is a constant and T_{cr} means the critical softening temperature (see Fig. 7). For TO_1 mode $A = 7.8$, T_{cr} is 1044 K and T_{cr} corresponds to Burns temperature T_d. For TO_2 mode obtained parameters is $T_{cr} = 1922$, $A = 37.7$.

CONCLUSIONS

- The dielectric properties of $0.2PbMg_{1/3}Nb_{2/3}O_3$-$0.4PbSc_{1/2}Nb_{1/2}O_3$-$0.4PbZn_{1/3}Nb_{2/3}O_3$ relaxors ceramics was investigated in very wide frequency 20 Hz $\leq \nu \leq$ 150 THz and temperature $20 \leq T \leq 500$ K region.
- Dielectric constant in the vicinity of the peak is very high (more than 14000) for 0.2PMN-0.4PSN-0.4PZN ceramics.
- Anomalous broad dielectric dispersion has been observed near the temperature T_m of maximum dielectric constant (at 1 kHz). The temperature dependencies of dielectric dispersion of present ceramics show typical relaxor behaviour.
- Distribution of relaxation times calculated directly from dielectric spectra. The broadening of spectra indicate a strong increase in inter-cluster correlation. Also the size of polar nano regions increases on cooling, at low temperatures the distribution of relaxation times has two maxima.
- In present ceramics two soft modes TO_1 and TO_2 have been observed. The TO_1 mode plays the role of the SM inside polar nanoclusters. The critical softening temperature T_{cr} of the TO_1 mode corresponds to Burns temperature T_d.

REFFERENCES

1. **Malibert, C.,et al** Order and Disorder in the Relaxor Ferroelectric Perovskite $PbSc_{1/2}Nb_{1/2}O_3$ (PSN): Comparison with Simple Perovskites $BaTiO_3$ and $PbTiO_3$ *J. Phys.: Condens. Matter*. 9 1997: pp. 7485 – 7500.
2. **Cheng, Z. Y., et al** Dielectric Behaviour of Lead Magnesium Niobate Relaxors *Phys. Rev. B* 55 (13) 1997: pp. 8165 – 8174.
3. **Perrin, C., et al** Neutron Diffraction Study of the Relaxor Ferroelectric Phase Transition in Disordered $PbSc_{1/2}Nb_{1/2}O_3$ *J. Phys.: Condens. Matter.* 12 2000: pp. 7523 – 7539.
4. **La-Orautapong, D., Toulouse, J., Robertson, J. L., Ye, Z. G.** Difuse Neutron Scattering Study of a Disordered Complex Perovskite $PbZn_{1/3}Nb_{2/3}O_3$ Crystal *Phys. Rev. B* 64 2001: 212101.
5. **De Mathan, N., et al** A Structural Model for the Relaxor PMN at 5 K *J. Phys.: Condens. Matter.* 3 1991: pp. 8159 – 8171.
6. **Pirc, R., Blinc, R.** Sperical Random Bond Random Field Model of Relaxor Ferroelectric *Phys. Rev. B* 60 (19) 1999: pp. 13470 – 13478.
7. **Raevski, I. P. et al.** Random-site Cation Ordering and Dielectric Properties of $PbMg_{1/3}Nb_{2/3}O_3$-$PbSc_{1/2}Nb_{1/2}O_3$ *Integrated Ferroelectrics* 53 2003: pp. 475 – 487.
8. **Dambekalne, M., Bormanis, K., Stenberg, A., Brandte, I.** Relaxor Ferroelectric $PbSc_{1/2}Nb_{1/2}O_3$-$PbZn_{1/3}Nb_{2/3}O_3$-$PbMg_{1/3}Nb_{2/3}O_3$ Ceramics *Ferroelectrics* 240 2000: pp. 221 – 228.
9. **Grigas, J.** Microwave Dielectric Spectroscopy of Ferro-electric and Related Materials. Gordon and Breach Science Publ., OPA Amsterdam, 1996.
10. **Pashkin, A., et al** THz Transmission Spectroscopy Applied to Dielectrics and Microwave Ceramics *Ferroelectrics* 254 2001: pp 113 – 120.
11. **Macutkevic, J., Banys, J., Matulis, A.** Determination of Distribution of Relaxation Times from Dielectric Spectra *Nonlinear Analysis: Modeling and Control* 9 (1) 2004: pp. 75 – 88.